Monthly Notices
of the
ROYAL ASTRONOMICAL SOCIETY

Mon. Not. R. Astron. Soc. **415,** 3006–3012 (2011) doi:10.1111/j.1365-2966.2011.18914.x

Photometric investigation of three W UMa-type binary stars in the old open cluster NGC 188

L. Liu,[1,2,3,4]★ S.-B. Qian,[1,2,3,4] L.-Y. Zhu,[1,2,3] J.-J. He,[1,2,3] W.-P. Liao,[1,2,3] L.-J. Li,[1,2,3,4] E.-G. Zhao[1,2,3,4] and J.-J. Wang[1,2,3,4]

[1]*National Astronomical Observatories/Yunnan Observatory, Chinese Academy of Sciences, PO Box 110, 650011 Kunming, China*
[2]*Key Laboratory for the Structure and Evolution of Celestial Objects, Chinese Academy of Sciences, 650011 Kunming, China*
[3]*United Laboratory of Optical Astronomy, Chinese Academy of Sciences (ULOAC), 100012 Beijing, China*
[4]*Graduate School of the CAS, Yuquan Road 19, Shijingshan Block, 100049 Beijing, China*

Accepted 2011 April 13. Received 2011 April 11; in original form 2011 March 12

ABSTRACT

In a programme to understand the evolution of contact binaries, we have re-observed EQ Cep, ER Cep and V371 Cep, which are members of the old open cluster NGC 188, photometrically. Combining our photometric solutions with some known parameters of the cluster, we derived the mass and the radius for each component. Meanwhile, we investigated the period changes of the three systems, finding a long-term increase of period in every system and discovering two cyclic variations in ER Cep besides the long-term changes ($T_3 = 5.40 \pm 0.01$ yr, $A_3 = 0.0135 \pm 0.0016$ d; $T_4 = 17.6 \pm 0.1$ yr). From the derived physical parameters and analysis of the orbital period, we conclude that (i) both components of V371 Cep have very possibly evolved off the main sequence, as a result of the derived accelerations of gravity $\log g_1 = 3.93$ and $\log g_2 = 3.98$, and (ii) ER Cep is at least a triple, or even quadruple, system, something suggested by the overmassive derived total mass ($\sim$3.51 $M_\odot$) and the 5.4-yr-cycle periodic oscillation.

Key words: binaries: close – binaries: eclipsing – stars: evolution – stars: individual: EQ Cep – stars: individual: ER Cep – stars: individual: V371 Cep.

1 INTRODUCTION

The old open cluster NGC 188 contains a large number of W UMa-type contact binaries. The first four were discovered by Hoffmeister (1964), and several more were found by Kaluzny & Shara (1987, hereafter KS87). In 1989, Kaluzny (1990, hereafter K90) re-observed them and published the *V*-band light curves of EQ Cep, ER Cep, ES Cep, V5, V6 and V7. In 1996, based on their new observations, Branly et al. (1996a, hereafter B96a) derived the basic parameters of EP Cep, EQ Cep, ER Cep, ES Cep and V369 Cep (V7) with the Wilson–Devinney (hereafter W–D) code. They found that EQ Cep, ER Cep and V369 Cep are contact binaries with a middle mass ratio and a low fill-out factor, whereas EP Cep and ES Cep seem to be near-contact binaries. Zhang et al. (2002, 2004, hereafter Z02 and Z04, respectively) again organized a survey to search for variable stars in NGC 188. There were 16 known W UMa-type binaries in NGC 188 after that programme.

The host, NGC 188, is an extensively studied old open cluster and not only provides an abundant population of contact binaries but also supplies many parameters for the environment that the contact binaries exist in. Fornal et al. (2007) gave a comprehensive list of parameters of NGC 188 in their table 1, including parameters such as the distance modulus, distance, age, $E(B-V)$ and [Fe/H]. From the table, we can see many different values of age, distance and so on. Based on the analysis of a solar-type double-lined eclipsing binary star (V12) in NGC 188, Meibom et al. (2009) derived a distance modulus of $(m-M)_V = 11.24 \pm 0.09$ mag, corresponding to 1770 ± 75 pc. They also determined an age of 6.2 ± 0.2 Gyr for NGC 188. Sarajedini et al. (1999) derived a value of 0.09 ± 0.02 for $E(B-V)$ by using a *UBVRI* CCD photometry method. As mentioned above, these parameters provide extremely extensive information for the study of contact binaries in the realm of NGC 188.

2 OBSERVATIONS

V-band observations of the NGC 188 field were carried out on three nights (2009 November 18 and 2010 December 25 and 30) with the 85-cm reflecting telescope at Xinglong Station of National Astronomical Observatories of the Chinese Academy of Sciences. The 1024 × 1024 PI1024 BFT CCD camera used yields a scale of 0.97 arcsec per pixel and a field of view of

★E-mail: LiuL@ynao.ac.cn

Table 1. Times of light minimum for EQ Cep.

JD+240 0000	Min.	Errors	E	$(O-C)$	Reference
46696.94504	p	0.00010	−28862	0.03911	K90
46775.66579	s	0.00017	−28605.5	0.02774	K90
46775.81843	p	0.00011	−28605	0.02690	K90
46778.73476	s	0.00008	−28595.5	0.02723	K90
51604.0470	p	0.0027	−12875	−0.03452	Z02
51605.1221	s	0.0021	−12871.5	−0.03374	Z02
51605.2749	p	0.0031	−12871	−0.03442	Z02
51811.2161	p	0.0028	−12200	−0.05524	Z02
51812.1248	p	0.0033	−12197	−0.06738	Z02
51813.0413	p	0.0027	−12194	−0.07172	Z02
55154.16493	s	0.00027	−1309.5	0.07782	our
55154.31821	p	0.00027	−1309	0.07762	our
55556.05512	p	0.00014	0	0.01977	our

16.5 arcmin × 16.5 arcmin. The filter system was a standard Johnson–Cousins–Bessel multicolour CCD photometric system built on the primary focus (Zhou et al. 2009). The V-band exposure times for each image were 300 s. 2MASS 00522551+8519275 and 2MASS 00495345+8517419 were chosen as comparison and check stars, respectively. The PSF (point spread function) method was used to reduce the observed images with IRAF. Five isolated and bright stars in each image were chosen as the PSF stars. From every observed image a PSF image was derived, which was used for the photometric magnitude corrections.

Since the times of light minima are symmetric, we used the least-squares parabolic fitting method to obtain several of them through our observations. The new obtained times of minima are listed in Tables 1–3.

3 PHOTOMETRIC SOLUTIONS WITH THE WILSON–DEVINNEY CODE

There were no published spectroscopic mass ratios of the three contact binaries, only the B96a-derived photometric mass ratios for the five excluding V371 Cep. This time, we only focused on the contact binaries. The 2003 version of the W–D program (Wilson & Devinney 1971; Wilson 1990, 1994; Wilson & Van Hamme 2003) was used to fit the light curves. During the solutions, the effective temperature of star 1, T_1, was fixed at the values described below. Also fixed at values chosen from the literature are the bolometric albedos A_1 and A_2, the gravity-darkening coefficients g_1 and g_2 and the limb-darkening coefficients of the V band. The quantities varied in the fitting are the mass ratio q, the effective temperature of star 2 T_2, the monochromatic luminosity of star 1 in each band L_1, the orbital inclination i and the dimensionless potential of star 1 Ω_1. Extensive testing revealed that EQ Cep, ER Cep and V371 Cep are contact systems, so the contact model was used in the final solutions (Mode 3, $\Omega_1 = \Omega_2$). The inputs and outputs are listed in Table 4.

Table 3. Times of light minimum for V371 Cep.

JD+240 0000	Min.	Errors	E	$(O-C)$	Reference
46696.8556	p	0.0007	−15127	0.00594	K90
46775.664	s	0.0008	−14992.5	−0.00080	K90
51605.052	p	0.0017	−6751	−0.01789	Z02
51813.0897	p	0.0008	−6396	−0.00528	Z02
55556.08769	s	0.00085	−8.5	0.00600	present paper
55561.06486	p	0.00088	0	0.00228	present paper

3.1 EQ Cep

$(B-V)$ for EQ Cep is 0.921 (K90) and the reddening $E(B-V)$ for NGC 188 is 0.09 (Sarajedini et al. 1999). Therefore, $(B-V)_0 = 0.831$ for EQ Cep if it is a member of NGC 188. With the well-known empirical relationship between colour index and temperature,

$$T = 8540/[(B-V)_0 + 0.865]\,\mathrm{K}, \quad (1)$$

the corresponding effective temperature is calculated as 5035 K. It must be pointed out here that the calculated value of the effective temperature depends sensitively on $(B-V)$ and $E(B-V)$; a small change in these will cause a large variation in the effective temperature. Actually, we had difficulty in estimating the effective

Table 2. Times of light minimum for ER Cep.

JD+240 0000	Min.	Errors	E	$(O-C)_1$	$(O-C)_2$	Reference
39237.410	p	0.001	−57128	0.01786	−0.00718	Kholopov & Sharov (1967)
41975.043	p	0.001	−47547	0.00441	−0.00175	Worden et al. (1978)
46434.68413	s	0.00066	−31939.5	0.00491	0.01464	KS87, Branly et al. (1996b)
46448.68333	s	0.00081	−31890.5	0.00299	0.01275	KS87, Branly et al. (1996b)
46696.98603	s	0.00007	−31021.5	0.00022	0.01032	K90
46775.70446	p	0.00007	−30746	−0.00190	0.00829	K90
46775.84883	s	0.00058	−30745.5	−0.00040	0.00979	K90
46778.70582	s	0.00019	−30735.5	−0.00078	0.00942	K90
46778.84774	p	0.00031	−30735	−0.00173	0.00847	K90
49888.79905	p	0.00028	−19851	−0.01221	−0.00279	Branly et al. (1996b)
49889.80016	s	0.00065	−19847.5	−0.01118	−0.00176	Branly et al. (1996b)
49890.9423	s	0.0012	−19843.5	−0.01199	−0.00257	Branly et al. 1996b
51811.2380	p	0.0018	−13123	−0.01197	−0.00751	Z02
51812.0956	p	0.0018	−13120	−0.01158	−0.00712	Z02
51813.0969	s	0.0026	−13116.5	−0.01036	−0.00591	Z02
55154.23247	s	0.00012	−1423.5	0.00216	−0.01014	the present paper
55556.12325	p	0.00020	−17	0.00382	−0.01120	the present paper
55560.98095	p	0.00021	0	0.00399	−0.01106	the present paper
55561.12347	s	0.00026	0.5	0.00364	−0.01141	the present paper

Table 4. Photometric solutions for the three contact binaries.

Parameters	EQ Cep	ER Cep	V371 Cep
$g_1 = g_2$	0.32	0.32	0.32
$A_1 = A_2$	0.50	1.00	0.50
$x_{1\mathrm{bolo}} = x_{2\mathrm{bolo}}$	0.292	0.255	0.293
$y_{1\mathrm{bolo}} = y_{2\mathrm{bolo}}$	0.407	0.452	0.405
$x_{1V} = x_{2V}$	0.026	0.016	0.391
$y_{1V} = y_{2V}$	0.039	0.187	0.103
T_1	5035 K	5321 K	5024 K
q	1.90 ± 0.04	2.22 ± 0.03	1.94 ± 0.02
Ω_{in}	5.1096	5.5600	5.1664
Ω_{out}	4.5156	4.9566	4.5712
T_2	4924 ± 16 K	5089 ± 15 K	4801 ± 65 K
i (°)	88.2 ± 1.9	83.5 ± 0.7	56.5 ± 0.7
$L_1/(L_1 + L_2)(V)$	0.3997 ± 0.0060	0.3935 ± 0.0046	0.3997 ± 0.0060
$\Omega_1 = \Omega_2$	4.7407 ± 0.0554	5.1860 ± 0.0442	4.9047 ± 0.0413
r_1(pole)	0.3403 ± 0.0070	0.3252 ± 0.0052	0.3270 ± 0.0046
r_1(side)	0.3623 ± 0.0092	0.3454 ± 0.0068	0.3457 ± 0.0058
r_1(back)	0.4310 ± 0.0222	0.4124 ± 0.0166	0.3988 ± 0.0113
r_2(pole)	0.4449 ± 0.0058	0.4544 ± 0.0041	0.4356 ± 0.0040
r_2(side)	0.4813 ± 0.0082	0.4924 ± 0.0058	0.4683 ± 0.0054
r_2(back)	0.5281 ± 0.0128	0.5352 ± 0.0088	0.5077 ± 0.0079
f	62.1 ± 9.3 per cent	62.0 ± 7.3 per cent	44.0 ± 6.9 per cent
θ (°)		89.95 ± 3.6	
ψ (°)		307.9 ± 2.3	
r_{spot} (°)		10.9 ± 1.4	
T_{s}/T_*		1.2 ± 0.1	

temperature because of the relative uncertainties of these two parameters. Fortunately, in the W–D code the light curve depends much more sensitively on the ratio of the two T_{eff} values than on the individual T_{eff} (Yakut & Eggleton 2005). Thus the mass ratio, the inclination and the degree of contact are probably not much affected by uncertainties in T_{eff}. Hence, most of the time we need not worry about how large the uncertainty for the effective temperature might be in the DC program[1] of the W–D code. In our solution, T_1 was therefore fixed at the calculated value, 5035 K. Generally speaking, low-mass main-sequence stars have a radiative core with a convective envelope; in contrast, medium-mass stars have a convective core with a radiative envelope. We adopted the first case, so the bolometric albedos are $A_1 = A_2 = 0.5$ for the convective-equilibrium envelope (Rucinski 1969). Values of the gravity-darkening coefficient $g_1 = g_2 = 0.32$ (Lucy 1967) were used, which correspond to the common convective envelope of both components. According to Claret & Gimenez (1990), square-root limb-darkening coefficients were used for the V band. The main photometric results are $q = 1.90 \pm 0.04$, $T_2 = 4924 \pm 16$ K and $f = 62.1 \pm 9.3$ per cent (Table 4). These indicate that EQ Cep is a W-type, medium mass ratio, high-contact binary. The fitted light curve (the solid line) is shown in Fig. 1.

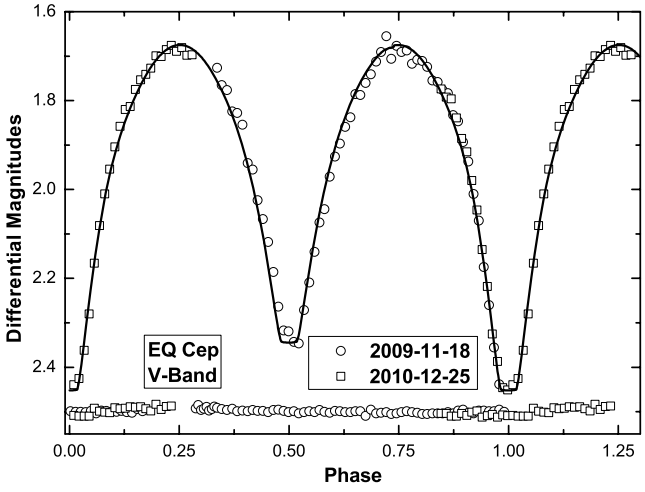

Figure 1. Observed light curves in the V band for EQ Cep. The phases were calculated by $245\,5154.31821 + 0.30694787 \times E$. The solid line denotes the theoretical light curve.

3.2 ER Cep

K90 gave $(B - V)$ as 0.830 for ER Cep. In the same way as for EQ Cep, the value of $(B - V)_0$ is calculated as 0.740 for ER Cep. The effective temperature of star 1, T_1, was fixed at 5321 K. The bolometric albedos, gravity-darkening coefficient, limb-darkening coefficients and mode of the W–D code are the same as for EQ Cep. The O'Connell effect (O'Connell 1951) in the light curve cannot be ignored. In consideration of the fact that ER Cep has mass transfer from the less massive component to the greater, a hot spot is introduced on the more massive component. The main photometric results are $q = 2.22 \pm 0.03$, $T_2 = 5089 \pm 15$ K, $f = 62.0 \pm 7.3$ per cent (Table 4). The fitted light curve (the solid line) is shown in Fig. 2. The introduced hot spot is displayed in Fig. 3.

[1] The DC program is a differential corrections main program (DC) for parameter adjustment of Light and velocity curves by the Least Squares criterion, and somewhat over two dozen subroutines used by both main programs.

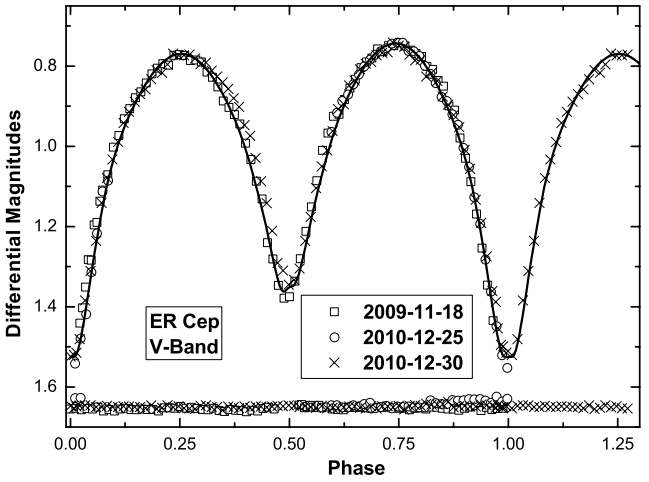

Figure 2. Observed light curves in the V band for ER Cep. The phases were calculated by 245 5154.23247 + 0.30694787 × E. The solid line denotes the theoretical light curve.

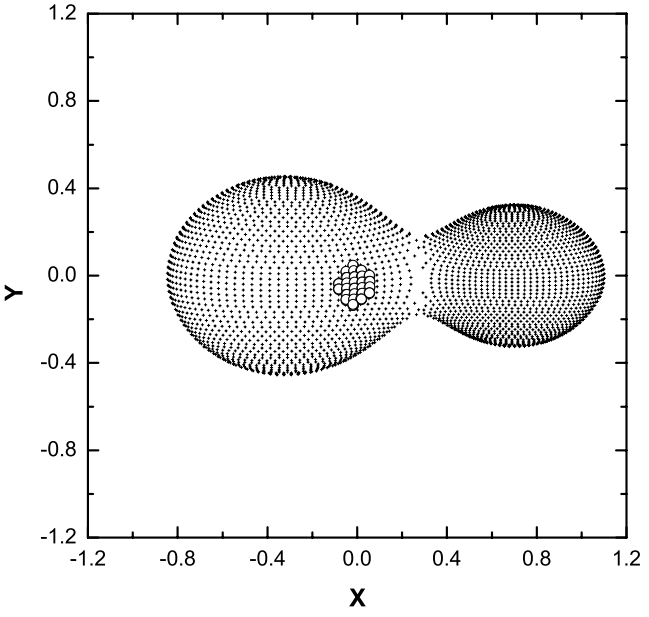

Figure 3. Geometrical structure of ER Cep at phase 0.75P, with a hot spot on the primary component.

3.3 V371 Cep

K90 gave $(B-V)$ as 0.925 for V371 Cep (V7). As for the previous systems, the value of $(B-V)_0$ is calculated as 0.835, yielding a T_1 of 5024 K. The other inputs are listed in Table 4, and need no special introduction. The main photometric results are $q = 1.94 \pm 0.02, T_2 = 4801 \pm 65$ K, $f = 44.0 \pm 6.9$ per cent (Table 4). Correspondingly, the fitted light curve is shown in Fig. 4 as the solid line.

4 ESTIMATION OF PHYSICAL PARAMETERS

The above three contact binaries are members of NGC 188 (see KS87, K90, Z02 and Z04), especially ER Cep and V371 Cep. The proper-motion membership probability (PMP) of those two is larger than 0.88 according to Z02. Thus, based on the distance modulus

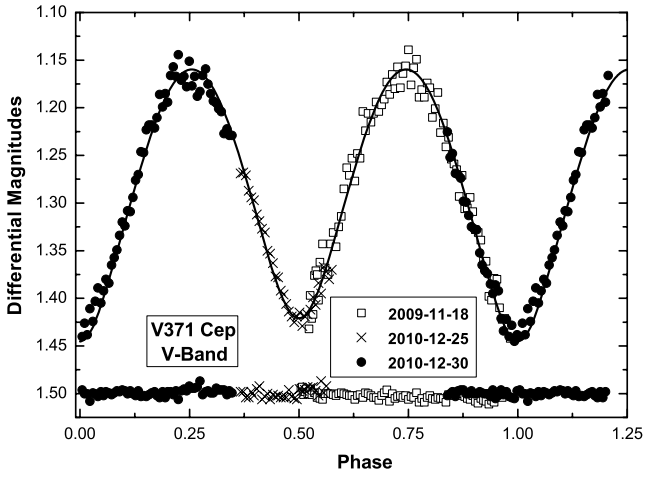

Figure 4. Observed light curves in the V band for V371 Cep. The phases were calculated by 245 5561.06486 + 0.58598612 × E. The solid line denotes the theoretical light curve as in Figs 1 and 2.

and the coefficient of light extinction in the V band of NGC 188 ($(m-M)_V = 11.24, A_v = 0.27$: Meibom et al. 2009), we compute the physical parameters of these three targets. The details are as follows.

First, we calculate the V-band absolute magnitude of the systems using $M_{V_{\max}} = m_{V_{\max}} - (\text{distance modulus})_V$. The maximum magnitude $m_{v_{\max}}$ appears at phase 0.25 or phase 0.75, when both surfaces of the two components face us. Each component contributes its luminosity to $M_{V_{\max}}$. Then, having considered bolometric corrections for $T_{\rm eff} = 5321$ K and $T_{\rm eff} = 5000$ K for the main-sequence stars in the V band (−0.26 mag for 5321 K and −0.4 mag for 5000 K: Schmidt-Kaler 1982), respectively, we obtain bolometric absolute magnitudes $M_{\rm bol}$ for the systems (4.80 mag for EQ Cep, 4.11 mag for ER Cep and 4.24 mag for V371 Cep, respectively). Secondly, we use the LC code[2] of the W–D program to estimate the combined bolometric absolute magnitudes, which can be compared with the results in the previous step. The LC code can provide $M_{\rm bol}$ values of each component from the period, semimajor axis and other parameters obtained from the photometric solutions. There is only one variable here, namely the semimajor axis. We take EQ Cep as an example. Every value of semimajor axis corresponds to a set of bolometric absolute magnitudes of star 1 and star 2. We add these to obtain the total value and find that when the semimajor axis is 2.18 solar radii, the bolometric absolute magnitudes of star 1 and star 2 are 5.81 and 5.35 mag, yielding $M_{\rm bol,max} = 4.803$ mag. This agrees with the observed value within the round-off errors. These inputs yield a set of physical parameters of EQ Cep, which are listed in Table 5. The parameters of ER Cep and V371 Cep obtained in the same way are also listed in Table 5.

According to the results of Meibom et al. (2009), the components of V12 are near to the main-sequence turn-off point (MSTOP) of NGC 188. Hence, the masses of the MSTOP stars should be larger than 1.1 $M_\odot$. Considering the deviations of probably 10 per cent that come from the uncertainty in the distance modulus (magnitudes), the total mass of ER Cep is greater than twice $M_{\rm TO}$.

[2] The LC code is used to generate light and radial velocity curves, spectral line profile, and images.

Table 5. Physical parameters for EQ Cep, ER Cep and V371 Cep.

	$M_1(\mathrm{M}_\odot)$	$M_2(\mathrm{M}_\odot)$	$R_1(\mathrm{R}_\odot)$	$R_2(\mathrm{R}_\odot)$	$A\ (\mathrm{R}_\odot)$	$\log g_1$ (cgs)	$\log g_2$ (cgs)	M_{bol1}	M_{bol2}	M_{bol}	$m_{v_{\max}}$
EQ Cep	0.51	0.97	0.82	1.06	2.18	4.32	4.37	5.81	5.35	4.803	16.44
ER Cep	1.09	2.42	1.00	1.37	2.77	4.48	4.55	5.15	4.65	4.119	15.61
V371 Cep	0.37	0.72	1.09	1.43	3.03	3.93	3.98	5.21	4.81	4.239	15.88

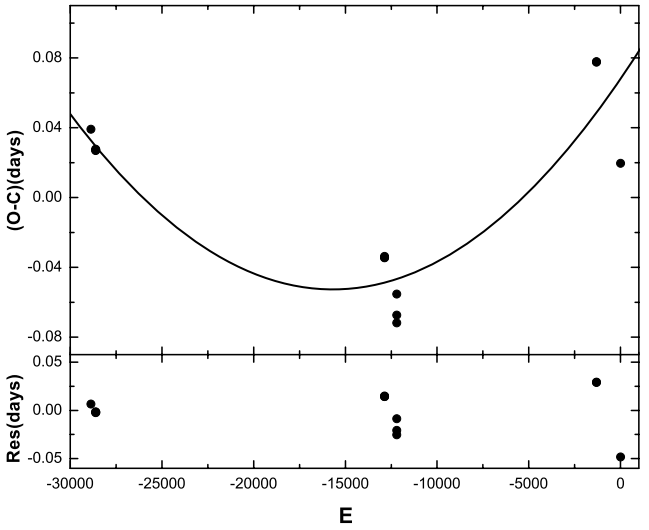

Figure 5. The $(O - C)$ diagram of EQ Cep. The $(O - C)$ values were computed by using a newly determined linear ephemeris (equation 2). The solid line represents the quadratic fitting (equation 3).

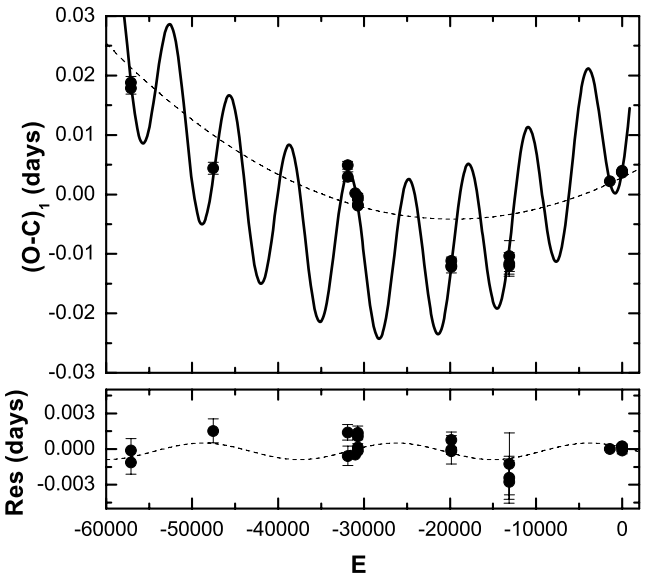

Figure 6. The $(O - C)$ diagram of ER Cep. The $(O - C)_1$ values were computed by using a newly determined linear ephemeris (equation 4). The solid line represents a quadratic fitting superimposed on a cyclic variation (equation 6). The dashed line in the upper panel represents the quadratic fit (equation 5). The lower panel plots the residuals for equation (6). The dashed line in this panel denotes another suspected much smaller period oscillation.

5 ORBITAL PERIOD VARIATIONS

The times of minima for the three contact binaries are enough to obtain a conclusion, even though there were only a few. We examine the $(O - C)$ diagram to investigate the orbital variations of the three systems, EQ Cep, ER Cep and V371 Cep.

5.1 EQ Cep

The first corrected period for EQ Cep was given by KS87. ZH02 contributed six times of minima. Superadded with ours, a total of 13 values were used to yield a new liner ephemeris,

$$\mathrm{Min.}\ I = 245\,5556.0354(81) + 0.30694787(86) \times E. \quad (2)$$

The $(O - C)$ values with respect to the linear ephemeris are listed in the fifth column of Table 1. The corresponding $(O - C)$ diagram is displayed in Fig. 5. It shows a long-term increase in the period. Hence, a quadratic ephemeris is yielded:

$$\mathrm{Min.}\ I = 245\,5556.1030(154) + 0.30696328(237) \times E + 4.90(73) \times 10^{-10} \times E^2. \quad (3)$$

With the quadratic term in this equation, the secular period increase rate is calculated to be $\mathrm{d}P/\mathrm{d}t = +1.17(\pm0.17) \times 10^{-6}\,\mathrm{day\,yr^{-1}}$.

5.2 ER Cep

This one is the most extensively studied target of the three. 20 times of minima were collected and are listed in Table 2. The time of minimum of 244 6450.6743 is not included here because it was determined using only four measurements (Branly et al. 1996b). The 20 measurements were used to yield a new liner ephemeris,

$$\mathrm{Min.}\ I = 245\,5560.9770(33) + 0.28573703(12) \times E. \quad (4)$$

The $(O - C)_1$ values with respect to the linear ephemeris are listed in the fifth column of Table 2. The corresponding $(O - C)_1$ diagram is displayed in Fig. 6. Because of the long-term increase trend, we used a quadratic ephemeris to fit the $(O - C)_1$ diagram. The result is

$$\mathrm{Min.}\ I = 245\,5560.9798(23) + 0.28573774(19) \times E + 1.81(33) \times 10^{-11} \times E^2. \quad (5)$$

The corresponding secular period increase rate is $\mathrm{d}P/\mathrm{d}t = +4.63(\pm0.84) \times 10^{-8}\,\mathrm{day\,yr^{-1}}$. However, this does not fit $(O - C)_1$ well (Fig. 6). Assuming that there is a cyclic oscillation in the period besides the long-term increase then, based on the formula in the format that follows, with the least-squares method, a much better fit is

$$\mathrm{Min.}\ I = 245\,5560.9921(62) + 0.28573901(51) \times E + 3.8(9) \times 10^{-11} \times E^2 + 0.0135(16)\sin[0.^\circ0521(1)E - 56.^\circ9(26.^\circ5)]. \quad (6)$$

With this fitting, the period for the oscillation is determined as 5.40 ± 0.01 yr and the final secular period increase rate is $\mathrm{d}P/\mathrm{d}t = +9.71(\pm2.30) \times 10^{-8}\,\mathrm{day\,yr^{-1}}$. Although this fits $(O - C)_1$ much better, weak evidence suggests that within the residuals exists another cyclic oscillation with a period possibly as high as 17.6 ± 0.1 yr. The corresponding $(O - C)_2$ values are shown in Fig. 7.

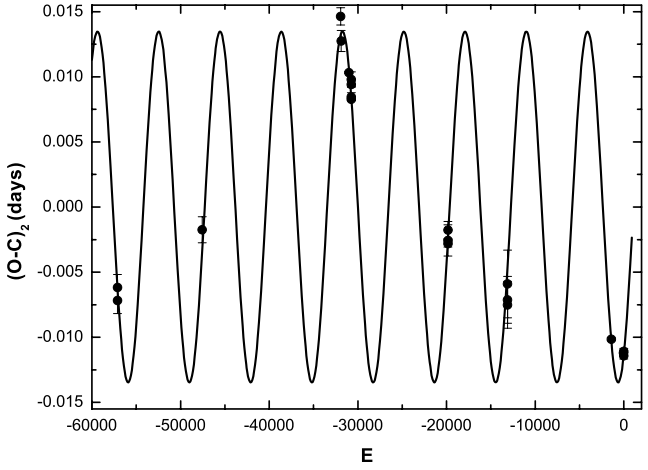

Figure 7. $(O - C)_2$ values for ER Cep with respect to the cyclic ephemeris in equation (6). The solid line represents the theoretical orbit of an assumed third body.

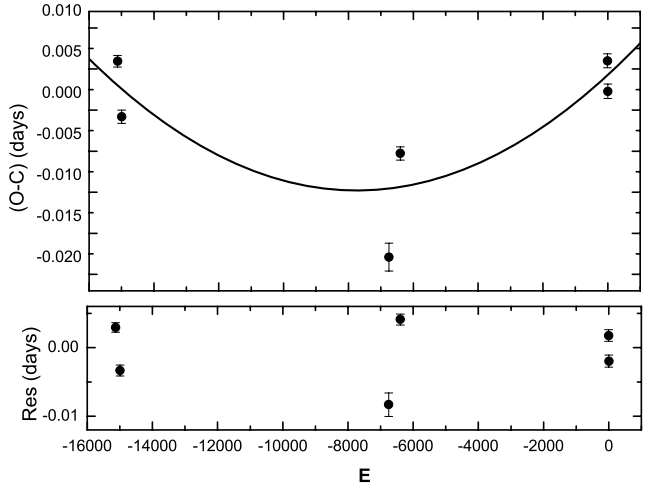

Figure 8. The $(O - C)$ diagram of V371 Cep. The $(O - C)$ values were computed by using a newly determined linear ephemeris (equation 7). The solid line represents the quadratic fitting (equation 8).

5.3 V371 Cep

Six available times of minima of V371 Cep are listed in Table 3. With them, a new liner ephemeris was yielded as

$$\text{Min. } I = 245\,5561.0626(65) + 0.58598612(68) \times E. \quad (7)$$

The $(O - C)$ values with respect to the linear ephemeris are listed in the fifth column of Table 3. The corresponding $(O - C)$ diagram is displayed in Fig. 8. A quadratic ephemeris was used to fit the $(O - C)$ diagram. The result is

$$\text{Min. } I = 245\,5561.06687(42) + 0.58598975(147) \times E + 2.35(91) \times 10^{-10} \times E^2, \quad (8)$$

implying a secular period increase with a rate of $\mathrm{d}P/\mathrm{d}t = +2.93\ (\pm 1.13) \times 10^{-7}\,\mathrm{day\,yr^{-1}}$.

6 DISCUSSION

Photometric solutions for the three contact binaries in NGC 188 were found. The photometric mass ratios for EQ Cep, ER Cep and V371 Cep are $1.90 \pm 0.04, 2.22 \pm 0.03$ and 1.94 ± 0.02, respectively. EQ Cep and ER Cep both have a high fill-out factor, 62.1 ± 9.3 and 62.0 ± 7.3 per cent, respectively, whereas V371 Cep has a medium fill-out factor, 44.0 ± 6.9 per cent. The values of the fill-out factors of EQ Cep and ER Cep are very different from those derived by B96a. This may be due to changes of the light curves. We estimated the masses and radii of all components: for EQ Cep, $M_1 = 0.51\,\mathrm{M}_\odot, M_2 = 0.97\,\mathrm{M}_\odot$; for ER Cep, $M_1 = 1.09\,\mathrm{M}_\odot, M_2 = 2.42\,\mathrm{M}_\odot$; for V371 Cep, $M_1 = 0.37\,\mathrm{M}_\odot, M_2 = 0.72\,\mathrm{M}_\odot$.

Through the period investigation, we find that all three systems show a long-term increase in period. Ordinarily, this period increase is thought of as conservative mass transfer from the less massive component to the more massive one. This type of mass transfer will cause the mass ratio to become progressively smaller and transfer angular momentum from the orbital to the primary component. When the orbital angular momentum is less than three times the total spin angular momentum, i.e. $J_{\mathrm{orb}} < 3J_{\mathrm{rot}}$ (Hut 1980), the two components will merge into a fast-rotation single star. The systems that have massive components should evolve into blue stragglers according to this mechanism. In order to understand the time-scales of this process, we estimated the mass transfer rates for the three systems using the well-known formula

$$\frac{\dot{P}}{P} = 3\frac{\dot{M}_2}{M_2}\left(\frac{M_2}{M_1} - 1\right). \quad (9)$$

The corresponding results are $\mathrm{d}M_1/\mathrm{d}t = -(1.37 \pm 0.20) \times 10^{-6}\,\mathrm{M}_\odot\,\mathrm{yr}^{-1}$ for EQ Cep, $\mathrm{d}M_1/\mathrm{d}t = -(2.25 \pm 0.53) \times 10^{-7}\,\mathrm{M}_\odot\,\mathrm{yr}^{-1}$ for ER Cep and $\mathrm{d}M_1/\mathrm{d}t = -(1.27 \pm 0.49) \times 10^{-7}\,\mathrm{M}_\odot\,\mathrm{yr}^{-1}$ for V371 Cep, respectively. The negative signs imply that the less massive component M_1 is losing mass. Therefore, if the less massive components keep these rates, the time-scales at which they completely lose their masses are 4.4×10^5 yr for EQ Cep, 4.8×10^6 yr for ER Cep and 2.9×10^6 yr for V371 Cep, respectively.

Advanced investigation reveals that the period of ER Cep may contain two cyclic oscillations ($T_3 = 5.40 \pm 0.01$ yr, $A_3 = 0.0135 \pm 0.0016$ day; $T_4 = 17.6 \pm 0.1$ yr). A cyclic oscillation is usually interpreted in two ways: the Applegate mechanism and the light-time effect. The Applegate mechanism says that the cyclic period change is caused by magnetic-activity-driven variations in the quadrupole moment of the solar-type components (e.g. Applegate 1992; Lanza, Rodonò & Rosner 1998). Alternatively, the light-time effect is a proposal that the cyclic period change is caused by orbital movement of the central system under the gravity of the third body. Considering the massive total mass ($\sim 3.51\,\mathrm{M}_\odot$) of ER Cep, we believe that it is a triple star at least. If the second oscillation is confirmed, it would be a quadruple star. An additional estimation of the mass of the third body is useless here before the spectroscopic mass ratios are obtained.

Through the solutions, we find that V371 Cep is also very special. The masses of its two components are much smaller than M_{TO}. The values for the acceleration of gravity at the surface of the components ($\log g_1 = 3.93$ and $\log g_2 = 3.98$) are distinct from the values for main-sequence stars. All of these suggest that both components of V371 Cep have evolved off the main sequence. This type of contact binary is quite rare. A star will expand when it evolved into the sub-giant stage. The components of ER Cep seem to be under this stage. However, because the inflation has not stopped yet, the system would be unstable. We believe that the two components of V371 Cep are pushing each other away, which ought to be reflected in its $(O - C)$ diagram. However, there are currently few times of minima available. Hence, it would be worth paying more attention to V371 Cep in the future.

ACKNOWLEDGMENTS

We especially appreciate the useful comments and cordial suggestions of W. van Rensbergen, which helped us to improve the paper greatly.

This work is partly supported by the Chinese Natural Science Foundation (No. 10973037 and No. 10903026), the National Key Fundamental Research Project through grant 2007CB815406, the Yunnan Natural Science Foundation (No. 2008CD157) and by West Light Foundation of the Chinese Academy of Sciences. New observations of the systems were obtained with the 85-cm telescope at Xinglong observation base.

REFERENCES

Applegate J. H., 1992, ApJ, 385, 621
Branly R. M., Athauda R. I., Fillingim M. O., van Hamme W., 1996a, Ap&SS, 235, 149
Branly R. M., Belfort M. E., Friend P. A., van Hamme W., Higgins R. J., 1996b, Inf. Bull. Variable Stars, No. 4374
Claret A., Gimenez A., 1990, A&A, 230, 412
Fornal B., Tucker D. L., Smith J. A., Allam S. S., Rider C. J., Sung H., 2007, AJ, 133, 1409
Hoffmeister C., 1964, Inf. Bull. Variable Stars, 67, 1
Hut P., 1980, A&A, 92, 167
Kholopov P. N., Sharov A. S., 1967, Astron. Tsirk, 426, 5
Kaluzny J., 1990, Acta Astron., 40, 61
Kaluzny J., Shara M. M., 1987, ApJ, 314, 585
Lanza A. F., Rodonò M., Rosner R., 1998, MNRAS, 296, 893
Lucy L. B., 1967, Z. Astrophys., 65, 89
Meibom S. et al., 2009, AJ, 137, 5086
O'Connell D. J. K., 1951, MNRAS, 111, 642
Rucinski S. M., 1969, Acta Astron., 19, 245
Sarajedini A., von Hippel T., Kozhurina-Platais V., Demarque P., 1999, AJ, 118, 2894
Schmidt-Kaler Th., 1982, in Schaifers K., Voigt H. H., eds, Landolt-Bornstein: Numerical Data and Functional Relationships in Science and Technology, Vol. 2b. Springer, Berlin
Wilson R. E., 1990, ApJ, 356, 613
Wilson R. E., 1994, PASP, 106, 921
Wilson R. E., Devinney E. J., 1971, ApJ, 166, 605
Wilson R. E., Van Hamme W., 2003, Computing Binary Stars Observables, 4th Edition of the W–D Program, available at ftp://ftp.astro.ufl.edu/pub/wilson/lcdc2003
Worden S. P., Coleman G. D., Rucinski S. M., Whelan J. A. J., 1978, MNRAS, 184, 33
Yakut K., Eggleton P. P., 2005, ApJ, 629, 1055
Zhang X. B., Deng L., Tian B., Zhou X., 2002, AJ, 123, 1548
Zhang X. B., Deng L., Zhou X., Xin Y., 2004, MNRAS, 355, 1369
Zhou A.-Y., Jiang X.-J., Zhang Y.-P., Wei J.-Y., 2009, Res. Astron. Astrophys., 9, 349

This paper has been typeset from a TEX/LATEX file prepared by the author.